ISSN 1682-296X (Print)
ISSN 1682-2978 (Online)

# Bio Technology

ANSInet
Asian Network for Scientific Information
308 Lasani Town, Sargodha Road, Faisalabad - Pakistan

Biotechnology 14 (3): 97-108, 2015
ISSN 1682-296X


ansinet
Asian Network for Scientific Information

RESEARCH ARTICLE OPEN ACCESS

DOI: 10.3923/biotech.2015.97.108

# Protective Effects of Highly Expressed Recombinant Human EC-SOD against ROS, UVB-Induced Apoptosis and DNA-Damage in Human Keratinocytes

[1,2]M.M. Muharram
[1]Department of Pharmacognosy, College of Pharmacy, Prince Sattam Bin Abdulaziz University, 11942, Alkharj, Kingdom of Saudi Arabia
[2]Department of Microbiology, College of Science, Al-Azhar University, Nasr City, 11884, Cairo, Egypt

ARTICLE INFO
*Article History:*
Received: February 08, 2015
Accepted: April 14, 2015

Corresponding Author:
M.M. Muharram,
Department of Pharmacognosy,
College of Pharmacy,
Prince Sattam Bin Abdulaziz University,
11942, Alkharj,
Kingdom of Saudi Arabia

ABSTRACT
Human extracellular superoxide dismutase (hEC-SOD) is a tetramer protein protects the extracellular space from oxidative stress by catalyzing the dismutation of biologically toxic superoxide anion into hydrogen peroxide and oxygen. Difficulty in obtaining large quantity of active recombinant (rhEC-SOD) has slowed its clinical applications although different systems have been used for its expression. In this study, transformed cells with His6-tagged rhEC-SOD were grown by fed-batch fermentation yielding a final dry weight of 16.47.6 g $L^{-1}$ as an inclusion body which comprised 43.17% of total protein. Inclusion bodies of the rhEC-SOD were solubilized, refolded and purified by Immobilized Metal Affinity (IMAC) and Gel Filtration Chromatography (GFC). With 2 L of fed-batch fermentation, 56 mg rhEC-SOD could be produced (purity 98%) with a total activity of 317.33 U. Appearance of the purified rhEC-SOD as a monomer form (26 kDa) directed the work to examine the role of the signal peptide at the N-terminal region in inducing the tetramer formation of this protein. In the predicted motif of the α-helix of the N-terminal region, amino acid substitutions of (M20D, V24D, W28A and V31D) lead to the complete disruption of the tetramer form of rhEC-SOD protein. However, no contribution could be detected with the mutations of (D12A, W16A and A22D). Partial disturbance of the tetramerization appeared with the mutations of R34A and I17D. Protective effects of rhEC-SOD against Reactive Oxygen Species (ROS), UVB-Induced apoptosis and DNA fragmentation were analyzed in human HaCaT keratinocytes. The rhEC-SOD had a scavenging activity of 30 and 14% against $H_2O_2$-induced ROS and UVB-induced ROS, respectively. Also, rhEC-SOD could reduce the UVB-induced nuclear fragmentation index from 21-9 (43%). In addition, the DNA damage and fragmentation index decreased from 1.54-1.15 in UVB irradiated upon the treatment of keratinocyte HaCaT cells with rhEC-SOD protein before UVB irradiation.

**Key words:** Extracellular superoxide dismutase, expression, fed-batch fermentation, tetramer, N-terminal domain, ROS, UVB, HaCaT keratinocytes, DNA-Damage, apoptosis

## INTRODUCTION

Reactive Oxygen Species (ROS) are produced by the cells as a metabolic by product and for the signaling of certain cellular processes (Nozik-Grayck *et al*., 2005). ROS describes free radicals, such as superoxide anion ($O^{2-}$), hydroxyl radical ($OH^-$) and other non-radical oxygen derivatives, such as hydrogen peroxide ($H_2O_2$) and hypochlorous acid (HClO). ROS can cause damage to DNA, lipids and protein when left unchecked (Halliwell, 1994; Stadtman and Levine, 2000; Forsberg *et al*., 2001; Cooke *et al*., 2003). They are closely related to a wide range of degenerative processes (Orr and

Sohal, 1994) and numerous chronic human diseases including inflammation (Finkel, 2005; Rosanna and Salvatore, 2012), reperfusion damage of ischemic tissue (Hatori *et al*., 1992) and motor neuron degeneration (McCord, 1994).

Cells have developed an array of defense systems to protect itself from ROS, that include metal sequestering proteins, use of scavenger compounds such as vitamin C and E, glutathione and specialized antioxidant enzymes such as catalase, peroxidase and Superoxide Dismutase (SOD) (Miller, 2004). Superoxide dismutase enzymes are present in most aerobic organisms. They catalyze the disproportionation of the superoxide radical anion $O^{-2}$ in cellular processes detoxifying reactive oxygen species (Miller, 2004). A protective role for many antioxidant molecules and SOD enzymes has been demonstrated and therefore they have been considered as medicines in combating a wide range of diseases (Niwa, 1989; Maxwell, 1995; Rahman *et al*., 2009). Mammalian cells express three isoforms of SOD enzymes: The cytoplasmic Cu/ZnSOD (SOD1), the mitochondrial MnSOD (SOD2) and the extracellular Cu/ZnSOD (SOD3), all of which require catalytic metal (Cu or Mn) for their activation.

Extracellular Cu/ZnSOD enzyme (EC-SOD) is present in the extracellular matrix of mammalian tissues (Marklund, 1984; Oury *et al*., 1994). With minor species-specific differences, EC-SOD is a hydrophobic glycoprotein with molecular weight of approximately 135,000 kDa (Marklund, 1982). It is present as a tetramer in numerous species (Oury *et al*., 1996; Fattman *et al*., 2000) and occasionally found as a dimer (Gerlach *et al*., 1998). Expression of EC-SOD is cell and tissue specific and is prominent in heart, lung, blood vessels, placenta and kidney (Nozik-Grayck *et al*., 2005). It protects against oxidation of Low-density Lipoprotein (LDL) a major contributor to atherosclerosis (Takatsu *et al*., 2001). Reduced and disruption of EC-SOD localization or activity may contribute to coronary artery disease (Landmesser *et al*., 2000) and impaired vasodilatation in cardiovascular diseases (Faraci and Didion, 2004). In addition, EC-SOD plays an important role in a number of lung diseases (Oury *et al*., 2002). Difficulty in obtaining enough EC-SOD has slowed its clinical applications as a biomedicine.

This study aimed to generate human recombinant EC-SOD as His-tagged protein by insertion the gene encoding the mature human EC-SOD protein into the plasmid pET-28a(+). Also, the present study aimed to study the role of the N-terminal signal sequence of hEC-SOD in tetramerization of this protein by investigating the effect of different mutations in the N-terminal domain. The ability of rhEC-SOD protein to protect human HaCaT keratinocytes from ROS (either from $H_2O_2$ or UVB irradiation), UVB-induced apoptosis and DNA damage was among the aims of the study as well.

## MATERIALS AND METHODS

**Plasmid construction and cloning:** The pUC18 plasmid harboring a 1396 bp cDNA fragment encoding the human EC-SOD was used for the PCR amplification of the EC-SOD using the following oligonucleotides: 5'-TAGAATTCGGACGGGCGAGGA-3' and 5'-TACTCGAGTCACTCTGAGTGCT-3' as upstream and downstream primers. The *Xho*I and *Eco*RI PCR product was inserted into the pET-28a (+) plasmid to construct the pET-EC-SOD expression plasmid. The plasmid pET-EC-SOD was used for the transformation of *E. coli* cells of strains BL21 (DE3) and BLR (DE3).

**Construction of the mutant proteins of rhEC-SOD:** To carry out amino acid substitutions in the rhEC-SOD constructs, site-directed mutagenesis was conducted according to the methods of Kunkel (1985) and Maartensson *et al*. (1995). Oligonucleotide primers were prepared using the Applied Biosystems Synthesizer 392 DNA/RNA. Wizard™ Miniprep DNA purification system from Promega was used to prepare all plasmids of the mutant proteins. DNA sequencing using the chain-termination method of Sanger *et al*. (1977) for the entire coding region of the rhEC-SOD was used for the confirmation of the different mutants.

**Proteolysis of EC-SOD and amino acid sequencing-analysis:** Purified samples of EC-SOD were incubated with trypsin (1:0.2 molar ratios) at 37°C for 30 min. To inhibit trypsin, 0.1 mM 3, 4-dichloroisocoumarin (DCI) was added for 30 min at 25°C followed by sample analysis with SDS-PAGE and staining with Coomassie brilliant blue R-250. In the presence of 10 mM dithiothreitol, purified-proteolytic fragments of EC-SOD were subjected to SDS-PAGE analysis and then transferred to Immobilon-P transfer membranes (Millipore) for amino terminal sequence analysis (Matsudaira, 1987). Using an Applied Biosystems Model 477A, samples were analyzed by Edman degradation sequencer with on-line phenylthiohydantoin analysis employing an Applied Biosystems Model 120A HPLC.

**Fed-batch fermentation:** Hundred milliliter of Luria-Bertani (LB) medium (containing 50 μg $mL^{-1}$ kanamycin) was inoculated with *E. coli* cells and grown at 37°C. Inoculated LB was added through a 0.2 μm syringe filter to the initial fermentation medium and used for stock and seed cultures as a growth medium. Stock cultures (-70°C) were prepared by growing transformed cells of *E. coli* BL21 (DE3) with/pET28-EC-SOD to the mid-log phase in LB medium containing kanamycin (50 mg $L^{-1}$), followed by harvesting and resuspending cells in LB medium with 15% glycerol. Seed cultures were prepared by subculturing stock cultures in 10 mL LB medium in a flask at 30°C. The fed-batch fermentation medium was as follows: 5 g $L^{-1}$ yeast extract, 10 g $L^{-1}$ trypton, 5 g $L^{-1}$ $K_2HPO_4$ and 5 g $L^{-1}$ NaCl. After sterilization, 40 g $L^{-1}$ glucose as a carbon source, 1 mL $L^{-1}$ of a trace metal solution and 10 mM $MgSO_4$ and were added. Fed-batch was initiated by transferring seed cultures to a 2 L fermenter (Braun Biotech, PA, USA). The pH of the culture was maintained at 6.8 using ammonia (15%), dissolved oxygen was controlled at 30% by automatic agitation 500 rpm. After the glucose concentration reached close to 0.05%,

protein expression was induced by adding IPTG to a final concentration of 1 mM.

**Cell harvesting, lysis and inclusion body purification:** After adding IPTG to a final concentration of 1 mM, culture growth was continued at 37°C and 250 rpm for 3 h. The culture was centrifuged at 6000×g for 30 min, supernatant was removed and the pellet was washed by Tris buffer (100 mM Tris, pH 8.0, 10 mM EDTA, 100 mM NaCl). Washed cell pellet was collected by centrifuging at 15000×g for 30 min at 4°C and stored at -20°C. Using the TE buffer (50 mM Tris-HCl, 0.5% Triton X-100, 1 mM EDTA, pH 8.0) the cell pellet was resuspended for sonication on ice (30 sec per pulse and 2 sec interval between pulses). Cell-lysate was centrifuged at 14,600×g for 30 min and the pellet containing the inclusion bodies was resuspended in a washing buffer (20 mM Tris-HCl, 1% Triton X-100, pH 8.0) and incubated for 30 min at room temperature. Resuspended pellet was centrifuged again for 15 min at 9,600×g. To remove the Triton completely, pellet washed with TE buffer and distilled water twice, respectively. About 50 mg of purified inclusion body extract were solubilized in a buffer containing [50 mM Tris-HCl (pH 8.0), 8.0 M urea and 0.5 M dithiothreitol (DTT)] at room temperature for 2 h and centrifuged for 30 min at 14,600×g. Supernatant was collected and the protein solution was stored at 4°C. Using Bovine Serum Albumin (BSA) as a standard, the protein concentration was determined according to the method described by Bradford (1976).

**Immobilized Metal Affinity Chromatography (IMAC), Gel Filtration Chromatography (GFC) and protein refolding:** A sephadex G-25 system (15×1.0 cm column) containing 5 mL sephadex G-25 beads was used to remove DTT and the equilibration buffer was 50 mM Tris-HCl (pH 3.0) containing 8.0 M urea. One milliliter of protein solution was applied onto and the column was eluted with the equilibration buffer. Fractions were collected and the protein concentration was determined. Immobilized Metal Affinity was applied using the crude columns of HisTrap FF (GE Biosciences). The pre-equilibrated IMAC column with (50 mM Tris-HCl, pH 8.0, 3.0 mM GSH, 0.5 mM GSSG, 8.0 M urea) was used for loading protein samples at a flow rate of 1 mL $min^{-1}$. Then the column was washed again with 10 mL of the equilibration buffer till the absorbance baseline of UV was reached. Refolding of the bound protein was performed on-column using a linear urea gradient from 8.0-1.0 M, starting with the equilibration buffer and finishing with a buffer containing 50 mM Tris-HCl, pH 8.0, 3.0 mM GSH, 0.5 mM GSSG, 50 μM $ZnCl_2$, 100 μM $CuSO_4$ and 1 M urea. The flow rate was 0.6 mL $min^{-1}$ and the total gradient volume was 30 mL. Refolded rEC-SOD was eluted using renaturation buffer (1 M urea and 1 M imidazole), pH 8.0. The eluae pooled and concentrated by ultrafiltration using Vivaspin (MWCO = 5,000). The concentrated rEC-SOD was purified on a Superose 12 PC 3.2/30 column equilibrated with PBS buffer after the refolding step. Ribonuclease (Mw = 13,700), carbonic anhydrase (Mw = 29,000), ovalbumin (Mw = 43,000) and Conalbumin (Mw = 75,000), ovalbumin were loaded onto the column as calibration standards. Then profile of rECSOD was compared with the standards for its multimer formation and molecular weight confirmation.

**Cross-linking analyses of Ec-SOD:** For Interchain cross-linking of rEC-SOD disuccinimidyl suberate (DSS) (Pierce, Rockford, IL, U.S.A.) was used. Ten microliter DSS (20 mM in DMSO) were mixed with 40 μL of purified rEC-SOD (0.6 mg $mL^{-1}$ in PBS) and incubated at room temperature for 5 min. The 25 μL of 0.5 M Tris, pH 8.7 was used to stop the reaction.

**Size-exclusion chromatography:** The apparent molecular weight of the wild type and mutant proteins of the rhEC-SOD was estimated by size exclusion chromatography on a Superose column (12 HR 10/30, Pharmacia Biotech), using 0.15 M NaCl as eluant and 10 mM potassium phosphate, pH 7.6, an injection volume of 200 pL, an elution rate of 0.5 mL $min^{-1}$ and protein concentrations of 2 mg $mL^{-1}$. Column was calibrated using the following protein markers: Thyroglobulin (670 kDa), bovine immunoglobulin G (158 kDa), ovalbumin (44 kDa), equine myoglobin (17.5 kDa) and vitamin B 12 (1.35 kDa).

**HPTLC analysis:** HPTLC densitometric analysis was performed on 10×20 cm aluminium-backed plates coated with 0.2 mm layers of silica gel 60 $F_{254}$ (E-Merck, Germany). Samples were applied to the TLC plates as 6 mm bands using a Camag Automatic TLC Sampler 4 (ATS4) sample applicator (Switzerland) fitted with a Camag microlitre syringe. A constant application rate of 150 nL $sec^{-1}$ was used. Linear ascending development of the plates to a distance of 80 mm was performed with hexane:ethyl acetate 8:2 (%, v/v) as mobile phase in a Camag Automatic Developing Chamber 2 (ADC2) previously saturated with mobile phase vapour for 30 min at 22°C. After development, the plates were scanned at 289 nm using a Camag TLC scanner in absorbance mode, using the deuterium lamp. The slit dimensions were 4.00×0.45 mm and the scanning speed was 20 mm $sec^{-1}$ (Alam *et al*., 2014).

**Detection of ROS:** To estimate the ROS generated by either UVB radiation or $H_2O_2$ in HaCaT keratinocytes the method of DCF-DA was applied (Rosenkranz *et al*., 1992).

**Nuclear staining:** Firstly, cells of HaCaT were treated with rhEC-SOD (100 μg $mL^{-1}$) and then irradiated with UVB for 1 h. Secondly, the cells were incubated at 37°C for 24 h. Then, a DNA-specific fluorescent dye [(1.5 μL of Hoechst 33342 (10 mg $mL^{-1}$)] was applied to each well and cells were incubated at 37°C for 10 min. Stained cells were visualized using a fluorescence microscope equipped with a CoolSNAP-Pro color digital camera (Media Cybernetics, Rockville, MD, USA). Degree of nuclear condensation was evaluated, the number of apoptotic cells were quantified and apoptotic index was estimated.

**Estimation of cellular DNA fragmentation:** DNA fragmentation was examined by analyzing the extent of cytoplasmic histone-associated DNA fragmentation according to the manufacturer's instructions of the kit from Roche Diagnostics (Portland, USA).

**Comet assay:** Extent of oxidative DNA damage was examined using the alkaline comet assay (Singh, 2000). In this test, 0.5% low melting agarose was mixed with a suspension of HaCaT cells at 39°C. This mixture was spread on fully-frosted microscopic slide pre-coated with 1% normal melting agarose (NMA; 200 μL). Then slides were covered with 0.5% LMA (75 μL). After solidification of the agarose, slides were immersed in a lysis solution [(1% Trion X-100, 100 mM Na-EDTA, 2.5 M NaCl, 10 mM Tris and 10% dimethyl sulfoxide (DMSO), pH 10)] and incubated at 4°C at for one hour. Slides were then placed in a gel electrophoresis unit containing a buffer of (10 mM Na-EDTA (pH 13), 300 mM NaOH) for 40 min allow for DNA unwinding and the expression of the alkali-labile damage. An electrical field of 300 mA and 25 V was then applied at 4°C for 20 min to direct the negatively charged DNA molecules towards the anode. Slides were washed with a neutralizing buffer (0.4 M Tris, pH 7.5) 3 times at 5 min each time at 4°C, stained with propidium iodide (20 μg $mL^{-1}$, 75 μL) and examined by a fluorescence microscope equipped with a Komet 5.5 image analysis system.

**Miscellaneous:** All DNA manipulation protocols including the restriction analysis, fragment-electro-elution, ligation and sequencing were performed as described in the study of Sambrook *et al*. (1989). Expression of the recombinant protein and purification were investigated by SDS-PAGE as described by Laemmli (1970) and Western blots analysis according to Towbin *et al*. (1979).

## RESULTS

**Construction of the pet-EC-SOD expression plasmid:** Recombinant human EC-SOD (rhEC-SOD) was generated by PCR amplification using primers that excluded the signal sequence of the N-terminal region and heparin binding domain at the C-terminal. For cloning the rhEC-SOD, two restriction sites of *Eco*RI and *Xho*I were introduced into the upstream and downstream primers, respectively. Both sites were used to insert the PCR fragment into the linearized pET-28a (+) plasmid. The rhEC-SOD was fused to His tag at the N-terminal to facilitate detection and purification. Recombinant plasmid of hEC-SOD was introduced to the cells of BL21 (DE3) and BLR (DE3), as two different expression hosts and checked for its recombinant protein expression with and without IPTG induction. To compare the expression level of rhEC-SOD in both hosts, total proteins from bacterial lysates were analyzed by SDS-PAGE (Fig. 1a) and Western analyses (Fig. 1b).

SDS analysis revealed that the protein intensity of induced rhEC-SOD (Fig. 1a, Lanes 2 and 5) is significantly higher than the non-induced one (Fig. 1a, Lanes 3 and 4). A protein band at about 26 kDa was detected by western analysis in both of the induced and non-induced cells. Protein blotting supported the result of the SDS-PAGE, showed the role of IPTG induction and the difference between the two strains in the expression of the rhEC-SOD. To check the optimum concentration of IPTG for the expression rhEC-SOD in both hosts, transformed cells with the recombinant plasmid (pET28a-EC-SOD-His6) were induced by IPTG with concentrations ranged between 250 μM and 3 mM. The blotting data (Fig. 2) showed that the optimum IPTG concentration for rhEC-SOD expression was 1 mM (Fig. 2, Lane 3). Although both cells were IPTG induced with the same different concentrations, intensity of the expressed protein bands by BL21 (Fig. 2, upper panel) was higher than

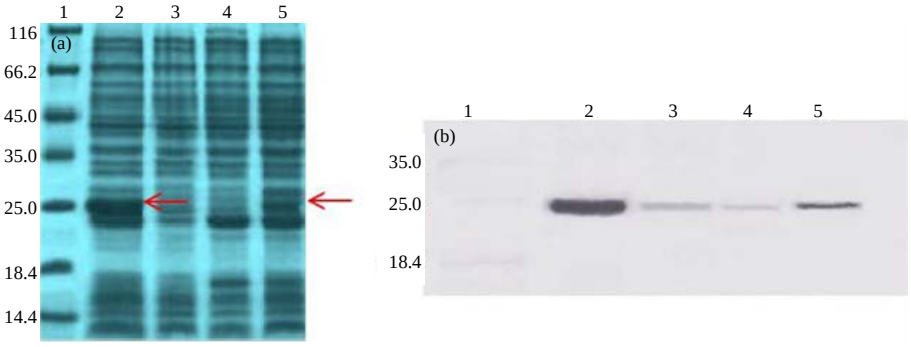


Fig. 1(a-b): Expression analysis of rhEC-SOD protein in *E. coli* cells of BL21 (DE3) and BLR (DE3) by (a) SDS-PAGE and (b) Western blot analysis. Lanes 1: Protein marker, Lanes 2: Induced cells of *E. coli* BL21 (DE3) with 1 mM IPTG; Lanes 3: Non-induced cells of *E. coli* BL21 (DE3), Lanes 4: Non-induced cells of *E. coli* BLR (DE3) and Lanes 5: Induced cells of BLR (DE3) with 1 mM IPTG. Arrows in (a) indicate to the predicted protein band of the rhEC-SOD at approximately 26 kDa. Proteins were examined in SDS-PAGE and Western blot analysis by Coomassie brilliant blue (R-250) and anti-His6 antibody, respectively

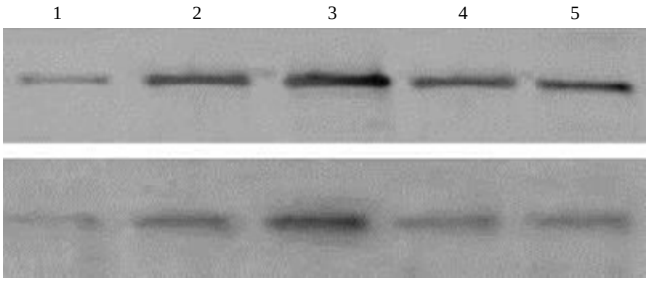


Fig. 2: Immunoblotting profile of rhEC-SOD with different concentrations of IPTG. Lanes 1-5: Represent induced protein of rhEC-SOD from *E. coli* cells [BL21 (DE3)-upper panel and BLR (DE3)-lower panel] with 250 µM, 500 µM, 1, 2 and 3 mM IPTG, respectively. Cells were cultured overnight at 37°C and 250 rpm on LB medium and their proteins were analyzed by Western analysis using anti-His6 antibody

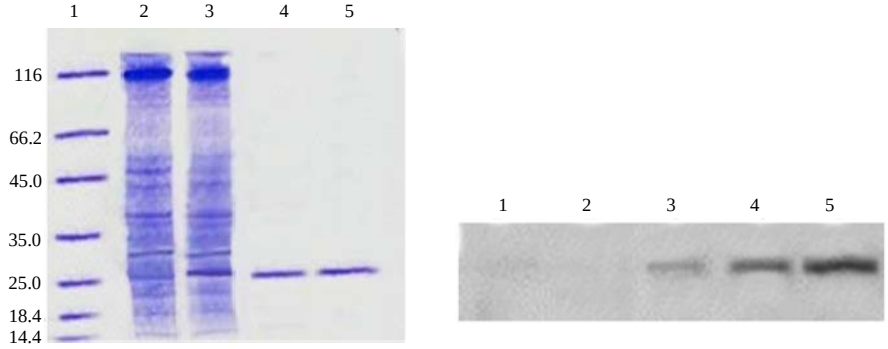


Fig. 3(a-b): Purification and refolding steps of rhEC-SOD (a) Stained SDS-PAGE with Coomassie Brilliant Blue showing the purification of rhEC-SOD and (b) Western blot analysis of purified rhEC-SOD. Lane 1: Protein marker, Lane 2: Total protein extract before induction, Lane 3: After induction, Lane 4: rhEC-SOD after refolding by $Ni^{2+}$ Sepharose column and Lane 5: rhEC-SOD after gel filtration column of superpose 12

that of BLR (DE3) (Fig. 2, lower panel). Therefore, cells of BL21 (DE3) strain were selected for the high expression of rhEC-SOD and further studies.

Expressed rEC-SOD in the induced cells was harvested as inclusion bodies. These inclusion bodies were then purified and renatured to yield biologically active rEC-SOD. To prepare the crude inclusion bodies of rEC-SOD, urea and Triton X-100 were used to remove native proteins and other soluble components of *E. coli*. Inclusion bodies were subsequently solubilized and loaded onto a column of $Ni^{2+}$ Sepharose. Urea was removed by washing the column, with urea gradient buffer containing glutathione (GSH) and oxidized glutathione (GSSG), to produce an active form of rEC-SOD. Metal ions of the $Cu^{2+}$ and $Zn^{2+}$ were important for higher activity recovery.

During the process of renaturation, the adsorbed rhEC-SOD protein was solid-phased refolded as attached to the resin surfaces by the dilution effect of urea and the reconstitution of the $Cu^{2+}$ and $Zn^{2+}$ metal ions. With a high concentration of $Cu^{2+}$ and $Zn^{2+}$ ions (250 mM), bounded rEC-SOD to the $Ni2^{+}$ Sepharose resin was released to the refolding buffer. Refolded protein was eluted and analyzed by SDS-PAGE and western analysis (Fig. 3). Data presented in Table 1 shows the different yields after each purification step of rhEC-SOD protein.

**Fed-batch fermentation of the rhEC-SOD:** To increase the productivity of rEC-SOD, transformed cells (BL21 (DE3) with pET-EC-SOD-His6) were initially grown on LB (containing kanamycin 50 mg $L^{-1}$) as growth medium and then cultured by fed-batch fermentation. Glucose was added to the feeding solution as a carbon source. To initiate the fed-batch fermentation, seeded cultures were transferred directly to a 2 L fermenter and 1 mM IPTG was used to induce the rEC-SOD after 10 h of fermentation. During fermentation the pattern of rEC-SOD expression was analyzed by SDS-PAGE of crude protein extracts at different time intervals (Fig. 4).

Production of rEC-SOD was increased dramatically after induction for a time period of 10 h after which there was no further increase. Cell growth continued and reached an optical density of 49.8 at $OD_{600}$ and a final dry cell weight of 16.47 g $L^{-1}$. The rEC-SOD ultimately comprised 43.17% of

Table 1: Yield of rhEC-SOD protein after purification

| Parameters | Total protein (g $L^{-1}$) | rhSC-SOD (g $L^{-1}$) | Total activity (U) | Purity (%) |
|---|---|---|---|---|
| Crude inclusion bodies (2 L) | 16.470 | - | - | - |
| After refolding | 2.960 | 2.400 | 2458.06 | 81 |
| After IMAC and GFC | 0.057 | 0.056 | 317.33 | 98 |

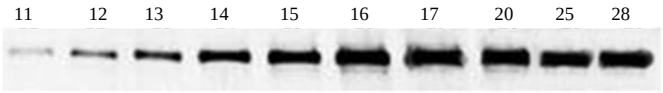


Fig. 4: Protein profile of the expressed rhEC-SOD by Western blot analysis at different time intervals (h)

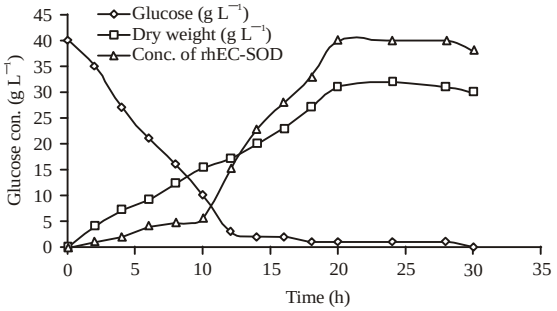


Fig. 5: Fermentation pattern of rEC-SOD against glucose concentration and dry weight of transformed bacterial cells

total. Inclusion bodies of the rhEC-SOD were solubilized, refolded and purified by Immobilized Metal Affinity (IMAC) and Gel Filtration Chromatography (GFC). With 2 L of fed-batch fermentation, 56 mg rhEC-SOD could be produced (purity 98%) with a total activity of 317.33 U (Table 1 and Fig. 5).

**Functional role of the N-terminal domain of EC-SOD:** Human EC-SOD is a tetramer protein of about 135 kDa (Oury *et al*., 1996; Fattman *et al*., 2000). In this study, analyzed protein profile of rhEC-SOD by SDS-PAGE and Western blot analysis was appeared only in the monomer form at about 26 kDa. This appearance was attributed to the exclusion of the heparin binding domain at the C-terminus. However, the signal peptide at the N-terminal region was also excluded in our construct which may reflect a role of this signal in inducing the tetramer formation as hypothesized from the methods of predicting secondary structure. In this hypothesis, the motif of (AEWIRDMYAKVTEIWQEV) in the N-terminal signal sequence of hEC-SOD seems to be involved in the formation of an amphipathic α-helical structure and might be involved in subunits interaction and formation of the tetramer form of EC-SOD protein.

To examine this hypothesis, different point of mutations were introduced by amino acid substitution in the predicted motif of the α-helix. At first, four different amino acid residues at positions I17 D, M20 D, V24 D and V31 D, respectively were substituted on the hydrophobic side of the α-helix. To test if any of the tryptophan residues plays any role in the formation of the tetramer, tryptophan residues at positions 16 and 28 were replaced by two alanine residues (W16A and W28A). Because the residues of the aspartate (D12) and arginine (R34) may play a role in the stabilization of the α-helix, they were replaced by two alanine residues although their position was outside the predicted sequence of the α-helix. Also, the alanine residue (A22) was replaced by aspartate because it is positioned in the middle at the charged-polar side of the α-helix. Mutants were verified by DNA-sequencing and their proteins were produced in *E. coli*, purified by affinity chromatography and examined for their effect on the tetramerization by blue native PAGE (Fig. 6) and size-exclusion chromatography analysis (Fig. 7).

Data presented in Fig. 6 and 7 shows the effect of mutation on the tetramerization of rhEC-SOD protein. These data can be classified into three categories. The first one (represented by the mutants, D12A, W16A and A22D) showed no effect on the oligomerization state compared to the native protein form. The second group (represented by the mutants, I17D and R34A) exhibited an oligomerization state ranged between monomer and tetramer form. Tetramer form was not shown in the third group (represented by the mutants, M20D. V24D, W28A and V31D) and their oligomerization pattern distributed between monomers and dimers.

Data of HPTLC densitometric analysis (Fig. 8) supported and confirmed the mutation effect on the tetramerization profile of rhEC-SOD protein (Fig. 8). Composition of the mobile was optimized to establish an accurate densitometric HPTLC procedure for the protein of rhEC-SOD. Used mobile phase [ethyl acetate-methanol-water 15:3:2 (%, v/v)] resulted in a well-resolved tetramer peak of the wild type of rhEc-SOD protein at $R_f$ value between 0.84 to 0.948±0.05) as shown in Fig. 8a. A single similar peak was appeared with the mutant proteins of DA12 (Fig. 8b) W16A

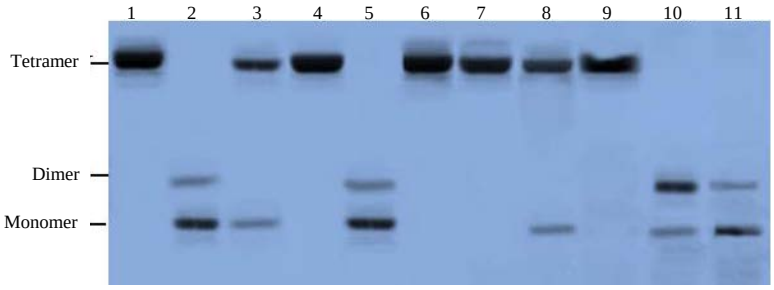


Fig. 6: Blue native PAGE for purified mutant proteins of the rhEC-SOD. Gel was stained with Coomassie brilliant blue (R-250). Lanes 1 and 6: Wild type protein of rhEC-SOD, Lanes 2-5: Protein of the mutants M20D, I17D, W16A and V24D, respectively. Lanes 7-11: Purified protein of the mutants D12A, R34A, A22D, V31D and W28A, respectively

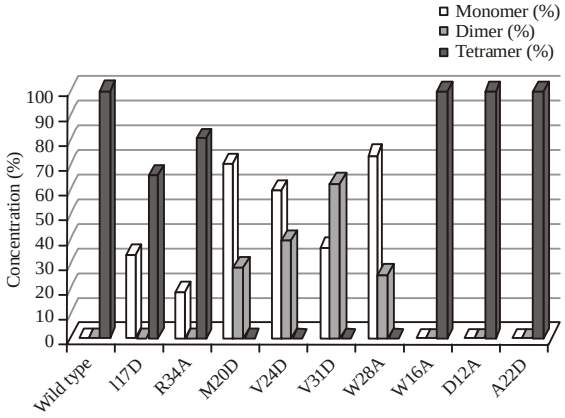


Fig. 7: Effect of mutation in the N-terminal domain on the tetramerization of rhEC-SOD based on size-exclusion chromatography on Superose 12

and A22D which confirmed that tetramerization was not affected by these mutations. However, tetramer and monomer peaks were developed with mutant proteins of R34A (Fig. 8c) and I17D . With the mutants of W28A (Fig. 8d) M20D, V24D and V31D, two resolved peaks were developed for the dimer and monomer forms. This confirmed that these mutations affected on rhEc-SOD tetramerization.

**Scavenging effect of rhEC-SOD protein against ROS:** Ultraviolet irradiation (UV), including UVA, UVB and UVC rays, causes numerous health problems. UVB irradiation is genotoxic and causing extensive cell damage. Many studies reported that UVB radiation induces ROS and leads to cell damage in epidermal keratinocytes. The rhEC-SOD protein was evaluated for its ability to scavenge induced ROS either from $H_2O_2$ or UVB in a concentration-dependent way. Compared with 67% activity for N-acetyl Cysteine (NAC), a well-known ROS scavenger that was used as a positive control, rhEC-SOD protein exhibited a scavenging activity against $H_2O_2$-induced ROS of 5, 8, 13, 27 and 30% at 25, 50, 100, 150 and 200 μg $mL^{-1}$, respectively. However, the scavenging activity of rhEC-SOD protein against UVB-induced ROS was 7% at 25 μg $mL^{-1}$, 10% at 50 μg $mL^{-1}$, 14% at 100 μg $mL^{-1}$, 9% at 150 μg $mL^{-1}$ and 7% at 200 μg $mL^{-1}$ compared with 28% for NAC (Fig. 9).

**Protective effect of rhEC-SOD protein against UVB-Induced apoptosis in human HACAT keratinocytes:** Many studies reported that irradiation of UVA and UVB can alter both enzymatic and non-enzymatic antioxidants which affect the antioxidant defense of the skin layers, increase ROS level can promote programmed cell death, apoptosis (Lawley *et al*., 2000; Rafferty *et al*., 2003; Sander *et al*., 2004).

Taken together, a significant fragmentation in cell-nuclei (indicated by arrows) was observed (apoptotic index, 21) with UVB irradiated keratinocyte cells (Fig. 10b) compared to intact nuclei of the control (Fig. 10a) cells. Interestingly, the nuclear fragmentation was markedly reduced (apoptotic index, 9.1) in UVB-irradiated HaCaT cells that were pretreated with treatment with rhEC-SOD protein (Fig. 10c). In addition, the index of the DNA damage and fragmentation was reduced from 1.54 in UVB irradiated keratinocyte cells (Fig. 11b) to 1.15 in HaCaT cells that were pretreated with rhEC-SOD protein before UVB irradiation (Fig. 11c).

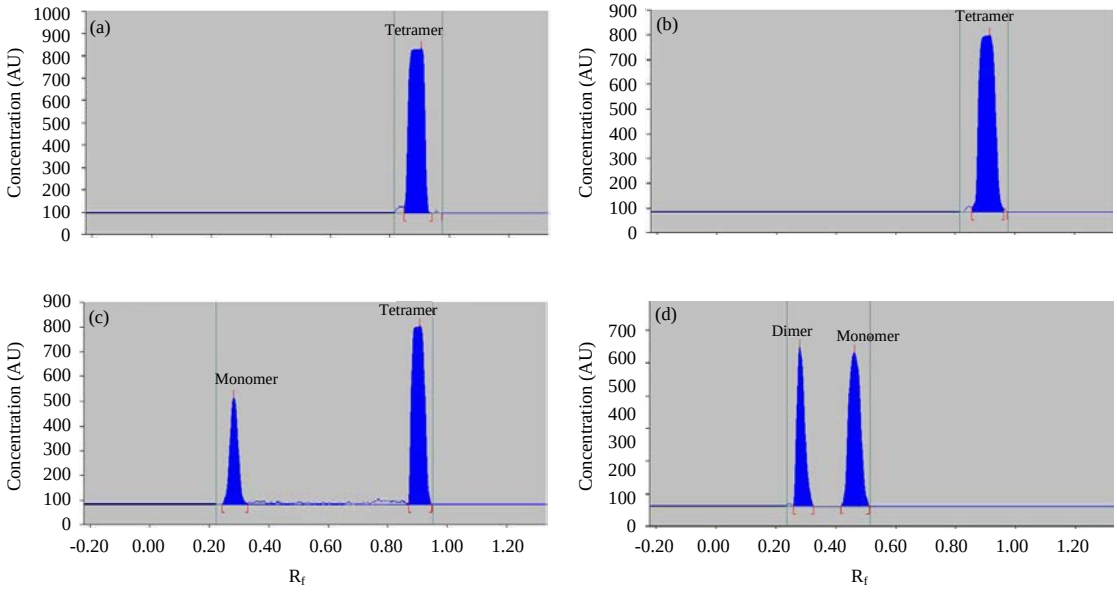


Fig. 8(a-d): HPTLC chromatogram of the purified protein of the (a) Wild type, (b) Purified proteins of the mutants DA12, (c) R34A and (d) W28A. Densitometric analysis was carried out at 254 nm

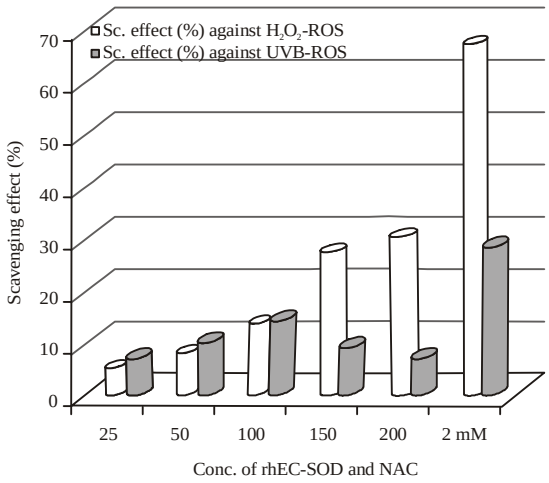


Fig. 9: Scavenging effect of rhEC-SOD protein against induced ROS either from $H_2O_2$ or UVB

## DISCUSSION

High costs for producing large quantities of recombinant human superoxide dismutase SOD3 (rhEC-SOD3) is a major obstacle to develop this enzyme as a biomedicine although different systems have been used for its expression (Petersen *et al*., 2005; Chen *et al*., 2006; Bae *et al*., 2013). Extracellular superoxide dismutase (EC-SOD) exhibits its own functions without cell penetration, since it is originally an extracellular antioxidant (Nozik-Grayck, 2005). Although different studies showed that rECSOD could be expressed in *E. coli*, it was expressed in an insoluble form as inclusion bodies and an *in vitro* refolding step was required to recover EC-SOD activity. In this study, a simple and easily reproducible method was applied for the preparation of rhEC-SOD. In this method, His6-tagged rEC-SOD was expressed under the control of the T7 promoter. It has been reported that the signal peptide of eukaryotes can associate onto membrane or produce an insoluble protein. Also, the C-terminus (heparin-binding domain of mature EC-SOD) can penetrate into the cell and target the nuclei. To overcome features of both terminals, plasmid of rEC-SOD was constructed without the signal sequence of the N-terminal region and heparin binding domain at the C-terminal. After IPTG induction, the expression strain (BL21 "DE3") efficiently produced the recombinant EC-SOD as revealed from SDS and western analyses. Inclusion bodies were solubilized, purified and loaded onto the column and the majority of them bound with $Ni^{2+}$ Sepharose. Denatured protein ECSOD was subjected to refolding on the IMAC column.

The overall fermentation process of rEC-SOD can be summarized in the following points: Fed batch fermentation of pET-EC-SOD transformed cells of BL21(DE3), expression of rEC-SOD as an inclusion body after IPTG induction, homogenization of cells, collection and refolding of rEC-SOD and purification steps. For a commercial production process, high-cell-density fermentation of recombinant protein is a primary prerequisite (Khalilzadeh *et al*., 2003). Also, this part of work showed that using of simple dilution refolding strategy was clearly superior to on-column refolding method and yielded highly purified rEC-SOD.

As mentioned before, hEC-SOD is present as a tetramer in numerous species (Oury *et al*., 1996; Fattman *et al*., 2000)

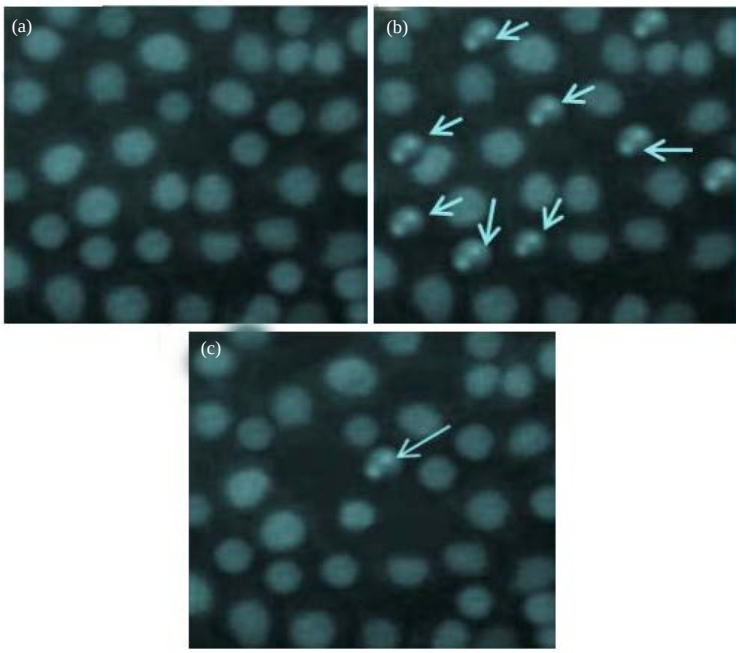


Fig. 10(a-c): Protective effect of rhEC-SOD protein against UVB-induced apoptosis in human HaCaT keratinocytes, (a) Control plate shows non irradiated cells, (b) Irradiated cells with UVB for 1 h and (c) Pretreated cells with rhEC-SOD protein (100 μg $mL^{-1}$) and exposed to UVB irradiation for 1 h. Formation of apoptotic bodies (indicted by arrows) was observed by staining the cells with Hoechst 33342 dye and fluorescence microscopy

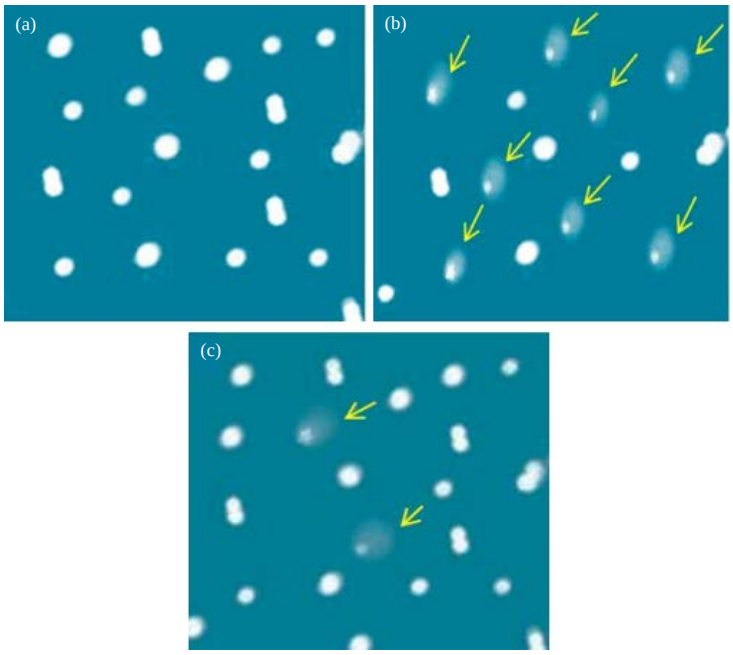


Fig. 11(a-c): Cytoplasmic histone-associated DNA fragmentation index, (a) None UVB-irradiated cells as a control, (b) One hour UVB irradiated HaCaT cells and (c) Pretreated HaCaT cells with rhEC-SOD prior UVB irradiation. Damage of cellular DNA was assessed by comet assay 24 h after irradiation of the HaCaT cells with UVB. Arrows indicate the fluorescence intensity in the tails of the comet-like structures

and occasionally found as a dimer (Gerlach *et al*., 1998). Formation of a disulfide bond between $Cys^{219}$ in two monomers leads to the dimerization of the EC-SOD (Oury *et al*., 1996; Fattman *et al*., 2003). Exclusion of the heparin binding domain at the C-terminus (absence of $Cys^{219}$) may reflect the detection of our recombinant protein only in the monomer form. However, the signal peptide at the N-terminal region was also excluded which confirm the role of this signal in inducing the tetramer formation. This hypothesis could be supported by a previous report (Tibell *et al*., 1996) that confirmed a role for the N-terminal domain of the hEC-SOD in the formation of three-dimensional structure and probably induces tetramer formation.

According to the results of amino acid substitutions, the α-helix motif at the N-terminal signal sequence of hEC-SOD is clearly involved in subunit interaction. This is because amino acid substitutions located on the hydrophobic side of the predicted α-helix (positions: M20D, V24D and V31D) lead to the complete disruption of the tetramer form (Fig. 6-8). No contribution could be detected for the replacement of amino acids located on the hydrophilic side of the N-terminal domain (D12A and A22D). This evidently confirmed that the hydrophilic side of the α-helix -helix has no role in the tetramerization. Mutation in positions (D12A and R34A) that were made to investigate effects of the a-helix stabilizing exhibited no importance with D12A because the rhEC-SOD variant appeared as 100% tetramer. However, substitution of arginine (R34A) has a destabilizing effect because this mutant exhibited a partial disturbance of the tetramerization (19% monomer and 81% tetramer) based on the data of size-exclusion chromatography (Fig. 7). The same partial destabilizing effect was noticed with (I17D) substitution (34% monomer and 66% tetramer). Because of the hydrophobic nature of aromatic amino acid residues that might help in shielding the contact area of the proposed hydrophobic tetramer, substitutions at positions W16A and W28A were made to clarify the role of the N-terminal tryptophan residues. Mutation of tryptophan residue at position 16 had no effect on the tetramerization whereas the replacement of (W28A) reflected an essential role for this residue. This role could be observed through its abolishing effect on the tetramerization. Interestingly, results of mutations in the N-terminal signal of the rhEC-SOD and their effect on the tetramerization of this protein were in harmony with the results of Stenlund *et al*. (1997) except for some variations in the results of the size-exclusion chromatography.

Irradiation of ultra violet has been considered as one of the most relevant environmental factors affecting human health (Karol, 2009; Narayanan *et al*., 2010). UVB radiation is genotoxic and causing extensive cell damage. Many studies reported that UVB radiation induces ROS and leads to cell damage in epidermal keratinocytes (Heck *et al*., 2003; Masaki *et al*., 2009). The present results demonstrated that the recombinant protein of EC-SOD had a scavenging activity reached to 30% against $H_2O_2$-induced ROS compared with 27% activity of *B. hamifera* extract (Piao *et al*., 2012) at the same concentration of 200 μg $mL^{-1}$ and 67% activity for N-acetyl cysteine (NAC). However, its scavenging activity against UVB-induced ROS was 14% at 100 μg $mL^{-1}$ compared with 28% for (NAC) suggesting that rhEC-SOD has effectively a quenching effect against ROS. Exposure to UVB leads to the generation of ROS, causing accumulation of modified protein carbonyls, damage to lipid membranes and DNA breaks (Ravanat *et al*., 2001; Davies and Truscott, 2001; Girotti, 2001) which may disrupt cellular function and contribute to apoptosis. In addition to the scavenging activity against ROS, rhEC-SOD could reduce the UVB-induced nuclear fragmentation index from 21-9. Approximately the same reduction value (43%) was achieved with *B. hamifera* extract, i.e., from 19.3-8.4 (Piao *et al*., 2012).

To ensure terminal differentiation and coordination throughout all layers of the human epidermis, a fine balancing should be maintained between keratinocyte proliferation and cell death (Mack *et al*., 2005). Upon disturbance of this balance by UVB irradiation, the cells will not be able to repair the resulting cellular damage (including DNA) which leads to apoptosis. Suppression of UVB-induced apoptosis in keratinocytes is beneficial for the prevention of photo-damage. In this study, it was also showed that DNA damage and fragmentation index decreased from 1.54 in UVB irradiated keratinocyte HaCaT cells (Fig. 11b) to 1.15 with pretreated HaCaT cells rhEC-SOD protein before UVB irradiation (Fig. 11c). Different pathways can be involved in UV-induced apoptosis including, activation of the tumor suppressor gene p53, autocrine release of death ligands, triggering of cell death receptors directly by UV and oxidative stress accompanied by mitochondrial changes and cytochrome c release (Kulms and Schwarz, 2000). Protection activity of rhEC-SOD against UVB-induced cell death may be exerted by interfering with one or more of these pathways.

## CONCLUSION

Recombinant human extracellular superoxide dismutase (rhEC-SOD) was expressed in *E. coli* cells of BL21 (DE3) using the $pET_{28}$hEC-SOD3 construct, produced with high-cell-density fermentation method and purified using a simple refolding protocol. Using site-directed mutagenesis, work was extended to investigate the nature role of the N-terminal domain of hEC-SOD in the induction of tetramerization. The protective effect of rhEC-SOD against ROS, UVB-Induced apoptosis and DNA fragmentation in human HaCaT keratinocytes was also investigated. Further work needs to be directed towards the protection mechanism of action of the rhEC-SOD protein.

## REFERENCES

Alam, P., A. Alam, K. Anwer and S.I. Alqasoumi, 2014. Quantitative estimation of hesperidin by HPTLC in different varieties of citrus peels. Asian Pac. J. Trop. Biomed., 4: 262-266.

Bae, J.Y., B.K. Koo, H.B. Ryu, J.A. Song and M.T. Nguyen *et al*., 2013. Cu/Zn incorporation during purification of soluble human EC-SOD from *E. coli* stabilizes proper disulfide bond formation. Applied Biochem. Biotechnol., 169: 1633-1647.

Bradford, M.M., 1976. A rapid and sensitive method for the quantitation of microgram quantities of protein utilizing the principle of protein-dye binding. Anal. Biochem., 72: 248-254.

Chen, H.L., C.C. Yen, T.C. Tsai, C.H. Yu and Y.J. Liou *et al*., 2006. Production and characterization of human extracellular superoxide dismutase in the methylotrophic yeast *Pichia pastoris*. J. Agric. Food Chem., 54: 8041-8047.

Cooke, M.S., M.D. Evans, M. Dizdaroglu and J. Lunec, 2003. Oxidative DNA damage: Mechanisms, mutation and disease. FASEB J., 17: 1195-1214.

Davies, M.J. and R.J.W. Truscott, 2001. Photo-oxidation of proteins and its role in cataractogenesis. J. Photochem. Photobiol. B: Biol., 63: 114-125.

Faraci, F.M. and S.P. Didion, 2004. Vascular protection: Superoxide dismutase isoforms in the vessel wall. Arteriosclerosis Thromb. Vasc. Biol., 24: 1367-1373.

Fattman, C.L., J.J. Enghild, J.D. Crapo, L.M. Schaefer, Z. Valnickova and T.D. Oury, 2000. Purification and characterization of extracellular superoxide dismutase in mouse lung. Biochem. Biophys. Res. Commun., 275: 542-548.

Fattman, C.L., L.M. Schaefer and T.D. Oury, 2003. Extracellular superoxide dismutase in biology and medicine. Free Radical Biol. Med., 35: 236-256.

Finkel, T., 2005. Radical medicine: Treating ageing to cure disease. Nat. Rev. Mol. Cell Biol., 6: 971-976.

Forsberg, L., U. de Faire and R. Morgenstern, 2001. Oxidative stress, human genetic variation and disease. Arch. Biochem. Biophys., 389: 84-93.

Gerlach, D., W. Reichardt and S. Vettermann, 1998. Extracellular superoxide dismutase from *Streptococcus pyogenes* type 12 strain is manganese-dependent. FEMS Microbiol. Lett., 160: 217-224.

Girotti, A.W., 2001. Photosensitized oxidation of membrane lipids: Reaction pathways, cytotoxic effects and cytoprotective mechanisms. J. Photochem. Photobiol. B: Biol., 63: 103-113.

Halliwell, B., 1994. Free radicals, antioxidants and human disease: Curiosity, cause, or consequence? Lancet, 344: 721-724.

Hatori, N., P.O. Sjoquist, S.L. Marklund, S.K. Pehrsson and L. Ryden, 1992. Effects of recombinant human extracellular-superoxide dismutase type C on myocardial reperfusion injury in isolated cold-arrested rat hearts. Free Radical Biol. Med., 13: 137-142.

Heck, D.E., A.M. Vetrano, T.M. Mariano and J.D. Laskin, 2003. UVB light stimulates production of reactive oxygen species: Unexpected role for catalase. J. Biol. Chem., 278: 22432-22436.

Karol, M.H., 2009. How environmental agents influence the aging process. Biomol. Ther., 17: 113-124.

Khalilzadeh, R., S.A. Shojaosadati, A. Bahrami and N. Maghsoudi, 2003. Over-expression of recombinant human interferon-gamma in high cell density fermentation of *Escherichia coli*. Biotechnol. Lett., 25: 1989-1992.

Kulms, D. and T. Schwarz, 2000. Molecular mechanisms of UV-induced apoptosis. Photodermatol. Photoimmunol. Photomed., 16: 195-201.

Kunkel, T.A., 1985. Rapid and efficient site-specific mutagenesis without phenotypic selection. Proc. Natl. Acad. Sci. USA., 82: 488-492.

Laemmli, U.K., 1970. Cleavage of structural proteins during the assembly of the head of bacteriophage T4. Nature, 227: 680-685.

Landmesser, U., R. Merten, S. Spiekermann, K. Buttner, H. Drexler and B. Hornig, 2000. Vascular extracellular superoxide dismutase activity in patients with coronary artery disease: Relation to endothelium-dependent vasodilation. Circulation, 101: 2264-2270.

Lawley, W., A. Doherty, S. Denniss, D. Chauhan and G. Pruijn *et al*., 2000. Rapid lupus autoantigen relocalization and reactive oxygen species accumulation following ultraviolet irradiation of human keratinocytes. Rheumatology, 39: 253-261.

Maartensson, L.G., P. Jonasson, P.O. Freskgaard, M. Svensson, U. Carlsson and B.H. Jonsson, 1995. Contribution of individual tryptophan residues to the fluorescence spectrum of native and denatured forms of human carbonic anhydrase II. Biochemistry, 34: 1011-1021.

Mack, J.A., S. Anand and E.V. Maytin, 2005. Proliferation and cornification during development of the mammalian epidermis. Birth Defects Res. Part C: Embryo Today: Rew., 75: 314-329.

Marklund, S.L., 1982. Human copper-containing superoxide dismutase of high molecular weight. Proc. Natl. Acad. Sci. USA., 79: 7634-7638.

Marklund, S.L., 1984. Extracellular superoxide dismutase in human tissues and human cell lines. J. Clin. Invest., 74: 1398-1403.

Masaki, H., Y. Izutsu, S. Yahagi and Y. Okano, 2009. Reactive oxygen species in HaCaT keratinocytes after UVB irradiation are triggered by intracellular $Ca^{2+}$ levels. J. Investig. Dermatol. Symp. Proc., 14: 50-52.

Matsudaira, P., 1987. Sequence from picomole quantities of proteins electroblotted onto polyvinylidene difluoride membranes. J. Biol. Chem., 262: 10035-10038.

Maxwell, S.R., 1995. Prospects for the use of antioxidant therapies. Drugs, 49: 345-361.

McCord, J.M., 1994. Mutant mice, Cu,Zn superoxide dismutase and motor neuron degeneration. Science, 266: 1586-1587.

Miller, A.F., 2004. Superoxide dismutases: Active sites that save, but a protein that kills. Curr. Opin. Chem. Biol., 8: 162-168.

Narayanan, D.L., R.N. Saladi and J.L. Fox, 2010. Review: Ultraviolet radiation and skin cancer. Int. J. Dermatol., 49: 978-986.

Niwa, Y., 1989. Lipid peroxides and superoxide dismutase (SOD) induction in skin inflammatory diseases and treatment with SOD preparations. Dermatologica, 179: 101-106.

Nozik-Grayck, E., H.B. Suliman and C.A. Piantadosi, 2005. Extracellular superoxide dismutase. Int. J. Biochem. Cell Biol., 37: 2466-2471.

Orr, W.C. and R.S. Sohal, 1994. Extension of life-span by overexpression of superoxide dismutase and catalase in Drosophila melanogaster. Science, 263: 1128-1130.

Oury, T.D., L.Y. Chang, S.L. Marklund, B.J. Day and J.D. Crapo, 1994. Immunocytochemical localization of extracellular superoxide dismutase in human lung. Lab. Invest., 70: 889-898.

Oury, T.D., J.D. Crapo, Z. Valnickova and J.J. Enghild, 1996. Human extracellular superoxide dismutase is a tetramer composed of two disulphide-linked dimers: A simplified, high-yield purification of extracellular superoxide dismutase. Biochem. J., 317: 51-57.

Oury, T.D., L.M. Schaefer, C.L. Fattman, A. Choi, K.E. Weck and S.C. Watkins, 2002. Depletion of pulmonary EC-SOD after exposure to hyperoxia. Am. J. Physiol. Lung Cell Mol. Physiol., 283: L777-L784.

Petersen, S.V., D.A. Olsen, J.M. Kenney, T.D. Oury and Z. Valnickova *et al*., 2005. The high concentration of $Arg^{213}$-->Gly extracellular superoxide dismutase (EC-SOD) in plasma is caused by a reduction of both heparin and collagen affinities. Biochem. J., 385: 427-432.

Piao, M.J., Y.J. Hyun, S.J. Cho, H.K. Kang and E.S. Yoo *et al*., 2012. An ethanol extract derived from *Bonnemaisonia hamifera* scavenges ultraviolet B (UVB) radiation-induced reactive oxygen species and attenuates UVB-induced cell damage in human keratinocytes. Mar. Drugs, 10: 2826-2845.

Rafferty, T.S., G.J. Beckett, C. Walker, Y.C. Bisset and R.C. McKenzie, 2003. Selenium protects primary human keratinocytes from apoptosis induced by exposure to ultraviolet radiation. Clin. Exp. Dermatol., 28: 294-300.

Rahman, N.A., K. Mori, M. Mizukami, T. Suzuki, N. Takahashi and C. Ohyama, 2009. Role of peroxynitrite and recombinant human manganese superoxide dismutase in reducing ischemia-reperfusion renal tissue injury. Trans. Proc., 41: 3603-3610.

Ravanat, J.L., T. Douki and J. Cadet, 2001. Direct and indirect effects of UV radiation on DNA and its components. J. Photochem. Photobiol. Biol., 63: 88-102.

Rosanna, D.P. and C. Salvatore, 2012. Reactive oxygen species, inflammation and lung diseases. Curr. Pharm. Des., 18: 3889-3900.

Rosenkranz, A.R., S. Schmaldienst, K.M. Stuhlmeier, W. Chen, W. Knapp and G.J. Zlabinger, 1992. A microplate assay for the detection of oxidative products using 2',7'-dichlorofluorescin-diacetate. J. Immunol. Meth., 156: 39-45.

Sambrook, J., E.F. Fritish and T. Maniatis, 1989. Molecular Cloning: A Laboratory Manual. 2nd Edn., Cold Spring Harbor Laboratory Press, New York, USA., ISBN-13: 978-0879693091, Pages: 3.

Sander, C.S., H. Chang, F. Hamm, P. Elsner and J.J. Thiele, 2004. Role of oxidative stress and the antioxidant network in cutaneous carcinogenesis. Int. J. Dermatol., 43: 326-335.

Sanger, F., S. Nicklen and A.R. Coulson, 1977. DNA sequencing with chain-terminating inhibitors. Proc. Natl. Acad. Sci., 74: 5463-5467.

Singh, N.P., 2000. Microgels for estimation of DNA strand breaks, DNA protein crosslinks and apoptosis. Mutat. Res., 455: 111-127.

Stadtman, E.R. and R.L. Levine, 2000. Protein oxidation. Ann. N.Y. Acad. Sci., 899: 191-208.

Stenlund, P., L.A.E. Tibell and D. Andersson, 1997. Subunit interaction in extracellular superoxide dismutase: Effects of mutations in the N-terminal domain. Protein Sci., 6: 2350-2358.

Takatsu, H., H. Tasaki, H.N. Kim, S. Ueda and M. Tsutsui *et al*., 2001. Overexpression of EC-SOD suppresses endothelial-cell-mediated LDL oxidation. Biochem. Biophys. Res. Commun., 285: 84-91.

Tibell, L.A.E., E. Skarfstad and B.H. Jonsson, 1996. Determination of the structural role of the N-terminal domain of human extracellular superoxide dismutase by use of protein fusions. Biochimica et Biophysica Acta (BBA)-Prot. Struct. Mol. Enzymol., 1292: 47-52.

Towbin, H., T. Staehelin and J. Gordon, 1979. Electrophoretic transfer of proteins from polyacrylamide gels to nitrocellulose sheets: Procedure and some applications. Proc. Natl. Acad. Sci. USA., 76: 4350-4354.